Letter

Parametrization of Catalytic Organic Reactions with Convex Hammett Plots

Jordi Ballesteros-Soberanas,[†] Cristina Bilanin,[†] and Antonio Leyva-Pérez*

Cite This: ACS Org. Inorg. Au 2023, 3, 13−18

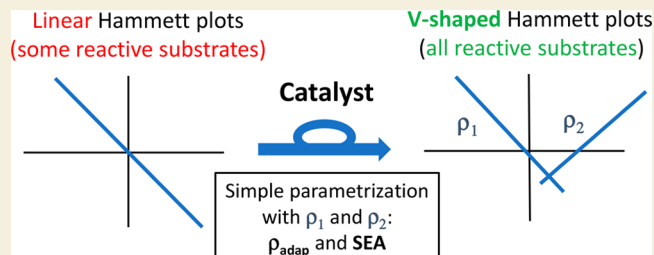Read Online

ACCESS | Metrics & More | Article Recommendations | Supporting Information

ABSTRACT: Quantification is essential to fairly compare between synthetic reactions in chemistry. Here we propose two new parameters called "adapted sensitivity constant" (ρ_{adap}) and "substrate electronics adaptability" (SEA), easily obtainable from Hammett plots, to assess the ability of a (catalytic) reaction to transform substrates with opposing electronics. These new parameters allow one to list reactions, catalyzed or not, as a function of substrate scope.

Linear Hammett plots (some reactive substrates) → Catalyst → V-shaped Hammett plots (all reactive substrates). ρ_1 ρ_2. Simple parametrization with ρ_1 and ρ_2: ρ_{adap} and SEA

■ INTRODUCTION

Parametrization of chemical reactivity is paramount for the advance of modern synthetic chemistry,[1,2] and the reactivity of a molecule is mainly controlled by the electron density of its functional groups. Figure 1A shows that the electronics—reactivity relationship in a given molecule is showcased by the Hammett equation, a free-energy relationship where the equilibrium constants or initial rates, relative to a reference substituent (usually the H atom), are correlated to the electron density of the reacting group, represented by σ values.[3] These σ values were calculated with a model reaction, i.e., benzoate hydrolysis, using substituents in the aromatic ring with different electron-donating or -withdrawing properties.[4] The corresponding Hammett plot is more often represented with the $\log(k/k_0)$, since initial rates provide information about electronic effects on the transition state (mechanistic information) compared to those based on equilibrium data (relative electronic effect on starting material and product). Besides, kinetic constants are easier to calculate experimentally than equilibrium constants. In any case, the values typically adjust to a straight line with a negative, neutral, or positive value of the slope, called sensitivity or, simply, reaction constant ρ. The sign of the constant ρ depends on the building of negative ($\rho > 1$) or positive charge ($\rho < 0$) in the transition state. However, an inflection of the line occurs in some cases, to give a convex (V-shaped) or concave (Λ-shaped) Hammett plot. The origin of the convex (V-shaped) Hammett plot comes from the occurrence of different processes concomitantly, but the extent to which they occur varies depending on the corresponding reaction rates, the presence of a catalyst or not, and the electronics of the substrate.[5] In contrast, concave downward Hammett plots represent a maximum value in the

electronics for a single reaction. In other words, while convex Hammett plots can be modified to widen the substrate scope, concave Hammett plots cannot.

Figure 1B shows a representative example of a convex Hammett plot reaction, i.e., the nucleophilic substitution reaction of benzyl derivatives.[6−8] Here, the transition state is composed by either benzylic carbocations stabilized by electron donor groups (EDGs) or poorly charged benzylic derivatives activated by electron-withdrawing groups (EWG), to which the nucleophile is finally added by a substitution reaction. This convex Hammett plot does not come from the action of any catalyst and is thus inherent to the substrates in play and unmodifiable. However, the use of a catalyst for other reactions can modify the reaction mechanism or boost one of the reactions in operando, thus transforming the regime from linear to nonlinear, provided that the mechanism of the reaction is controlled by the substrate—catalyst interaction. In other words, the choice of a proper catalyst can generate a convex Hammett plot, thus significantly expanding the substrate scope of the reaction.

It is difficult to find in the literature catalysts able to produce convex Hammett plots, and to our knowledge, only two catalytic systems have been reported in the last years.[4] The first one consists of Mn(V) complexes to catalyze hydride[9] and oxygen atom[10] transfer reactions, and the other makes use of
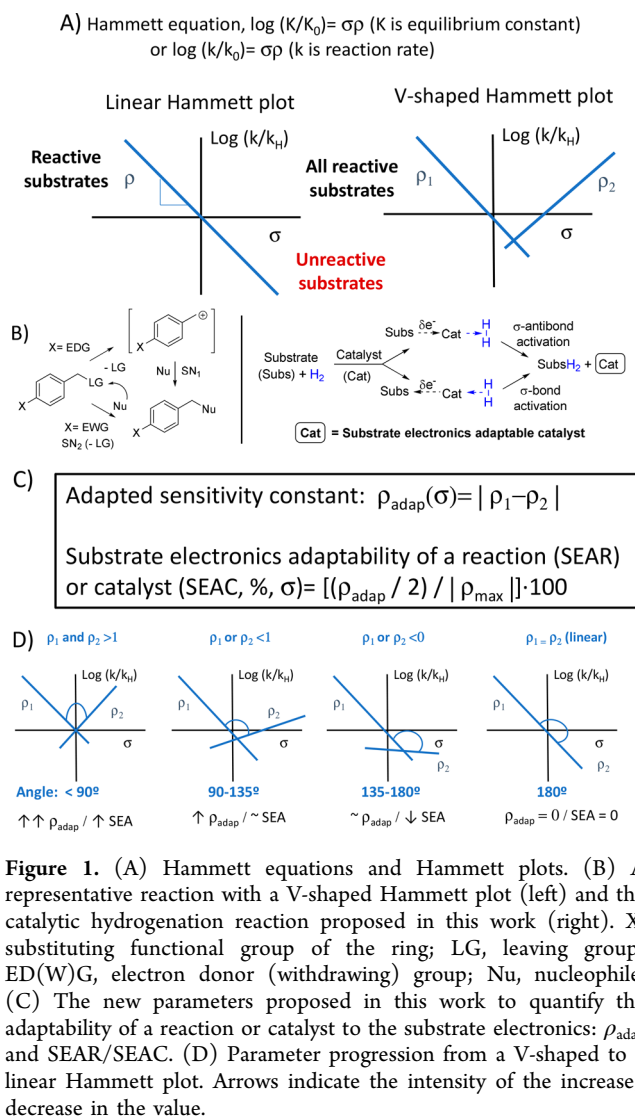
A) Hammett equation, log (K/K_0)= σρ (K is equilibrium constant)
or log (k/k_0)= σρ (k is reaction rate)

Figure 1. (A) Hammett equations and Hammett plots. (B) A representative reaction with a V-shaped Hammett plot (left) and the catalytic hydrogenation reaction proposed in this work (right). X, substituting functional group of the ring; LG, leaving group; ED(W)G, electron donor (withdrawing) group; Nu, nucleophile. (C) The new parameters proposed in this work to quantify the adaptability of a reaction or catalyst to the substrate electronics: ρ_{adap} and SEAR/SEAC. (D) Parameter progression from a V-shaped to a linear Hammett plot. Arrows indicate the intensity of the increase/decrease in the value.

Ru with differently substituted phenol ligands to catalyze the hydrogenolysis of ketones.[11] The latter incidentally describes but does not claim to parametrize the effect proposed here, i.e., the use of different catalysts to modulate the Hammett plot from linear to V-shaped, and shows that the V-shaped effect also occurs when the phenol compound is used as a reactant during the Ru-catalyzed coupling reaction with aldehydes.[12]

Figure 1B also shows our proposal here, which consists of catalysts able to generate V-shaped Hammett plots by changing the reaction mechanism, after interacting with substrates of opposed electronics. For instance, it is known[13,14] that the hydrogenation reaction proceeds either by populating the $1\sigma^*$ antibonding orbital of the H−H bond with electron density coming from electron-rich substrate−catalyst intermediates or, on the contrary, by extracting electron density from the 1σ bonding orbital of the same adduct with electron-withdrawing substrates, provided that the catalyst can manifold both mechanisms. Although the activation of diatomic molecules in these two ways is well-known,[15] particularly with H_2, the concomitant occurrence of both opposed mechanisms in a single catalyst can become a strategy to achieve a wide substrate scope after generation of a V-shaped Hammett plot. However, to our knowledge, this approach has not been explored yet.

■ RESULTS AND DISCUSSION

Figure 1C shows two new variables proposed here to quantify the impact of a mechanistic change on substrate scope, easily calculated from the V-shaped Hammett plot. We define "adapted sensitivity constant" (ρ_{adap}) as the difference between the slope values of the V-shaped line, and the formula can be written as follows: $\rho_{adap}(\sigma) = |\rho_1 - \rho_2|$, where σ denotes the tabulated values chosen to construct the Hammett plot (they can be different, i.e., σ^+ or σ^-, and it should be indicated). The slopes ρ_1 (left, toward more EDG) and ρ_2 (right, toward more EWG) define the two lines forming the V-shaped curves, in absolute value. The number ρ_{adap} can be easily obtained from the V-shaped graph and gives an estimation of the substrate scope achievable by a catalyst in terms of substrate electronics. The higher ρ_{adap} is, the wider the scope can potentially become.

We also propose here the parameter "substrate electronics adaptability" (SEA), either for an uncatalyzed (SEAR) or a catalyzed reaction (SEAC), to define how similar the reactivities of substrates with opposing electronics are. The parameter SEA is calculated by the formula SEA $(\%, \rho) = [(\rho_{adap}/2)/|\rho_{max}|] \times 100$, where ρ_{adap} is the adapted sensitivity constant defined above and ρ_{max} is the higher ρ value. Figure 1D depicts how this formula constitutes a simplified way to assess the angle formed by the V-shaped curve at the corner, in other words, how similar both mechanisms are. The higher the ρ_{adap} and SEA values, the better the reaction scope, since SEA = 100% corresponds to a symmetrically equal performance in the two regimes delimited by the Hammett plot and SEA = 0% corresponds to a linear Hammett plot (angle = 180°).

A more in-depth explanation in terms of kinetic and energetic parameters can be found in the Supporting Information (Figure S1). ρ_{adap} expresses the sum of the contribution in lowering the activation energies from both regimes delineated by the Hammett plot, compared to the vertex of the plot using only Hammett parameters, and is proportional to the rate of change of the activation energies with respect to the electronic value (σ). Thus, ρ_{adap} becomes zero when the Hammett plot is a straight line and grows larger when sharp V-shaped Hammett plots occur. Equation 1 defines these values:

$$\rho_{adap} = |\rho_1 - \rho_2| = \left| \frac{\Delta Ea_1/\sigma_1 - \Delta Ea_2/\sigma_2}{RT} \right| \qquad (1)$$

σ_1 is always negative when the vertex is σ_H; σ_2 is always positive when the vertex is σ_H; ΔEa_x is always positive if the reaction is faster than with a p-H aromatic derivative (see Figure S1).

SEA expresses the ratio of the activation energy change rate with respect to the electronic value (σ) of the two regimes delineated by the V-shaped Hammett plot, thus indicating how comparable both regimes are in terms of the change in activation energies using only Hammett parameters. The equation itself already hints at the fact that, if $\rho_1 \geq 0$, namely, the slope on the EDG is positive or zero, the maximum value of SEA is 0.5. Equation 2 defines these values (see Figure S1 for details).

If $|\Delta Ea_1| > |\Delta Ea_2|$: $SEA = \dfrac{1}{2}\left|1 + \dfrac{\sigma_1}{\sigma_2}\dfrac{\Delta Ea_2}{\Delta Ea_1}\right|, \quad 0 \leq SEA \leq 1$

If $|\Delta Ea_2| > |\Delta Ea_1|$: $SEA = \dfrac{1}{2}\left|\dfrac{\sigma_2}{\sigma_1}\dfrac{\Delta Ea_1}{\Delta Ea_2} - 1\right|, \quad 0 \leq SEA \leq 0.5$

$$(2)$$

With these proposed variables, ρ_{adap} and SEA, in hand, one can quantify, tabulate, and compare different reactions showing V-shaped Hammett plots, catalyzed or not. For the sake of illustration, the calculated values of ρ_{adap} and SEAC for the few catalytic examples found in the literature (Table S1) and also for a variety of uncatalyzed organic reactions (Table S2) have been listed. It can be seen that $\rho_{adap} \sim 5$ and SEAC = 95% can be obtained for catalyzed reactions, competing with uncatalyzed reactions. These high values of ρ_{adap} and SEAC mean that a catalyst can react with a wide range of substrates regardless of the electronics, enabling a high diversity of products. It is worth commenting here that both parameters, ρ_{adap} and SEA, denote slightly different effects: the former quantifies the range of substrates to react and the abruptness of the mechanism change, and the latter denotes the similarity between both electronic regimes.

It could be thought that V-shaped Hammett plots are bizarre, but they might be more general than reported. Researchers may be tempted to discard the extreme points in Hammett plots when they dramatically differ from linearity, and it could very well occur that some "truncated" V-shaped Hammett plots are present in the literature. This is more plausible when considering that a plethora of modern catalyzed methods show very wide scopes; thus, these catalysts could be adaptable and give V-shaped Hammett plots. It is true that a very active catalyst can cover the whole electronic range without requiring an inflection in the curve,; however, a V-shaped line better homogenizes the reactivity of substrates with opposing electronics. The need for wide substrate scopes, covering the diverse electronic range of organic molecules, becomes absolutely necessary when considering that the most influencing functional groups in biologically active molecules are not only (tertiary) amines and ethers (strong electron donors) but also trifluoromethyl, chloro, fluoro, and cyano groups (strong electron-withdrawing groups).[16] As a matter of fact, some of the discrete organic molecules (not monoclonal antibodies or biologic medical products) which rank first among blockbuster drugs contain these electronically biased functional groups (Figure S2).[17]

Two reactions are studied here as a proof-of-concept for the new parameters. Figure 2 shows the Hammett plot for the Pd-catalyzed semi-hydrogenation reaction of different terminal alkynes to alkenes.[18] Three different Pd catalysts were used: the current industrial Lindlar (Pd–Pb nanoparticles supported on CaCO$_3$) catalyst,[19] a commercially available BASF colloidal Pd nanoparticulated catalyst (c-Pd/TiS),[20] and a house-made catalyst composed of ultrasmall Pd clusters on CaCO$_3$ nanoparticles $[Pd-(CaCO_3)_n]$.[21,22] The latter combines the chemical composition of the Lindlar catalyst (Pd on CaCO$_3$ sites)[23] with the nanoparticulated structure of the c-Pd/TiS catalyst, free of Pb,[24] confirmed by electron microscopy imaging (Figures S3–S5). The points in the Hammett plots were replicated three times in order to properly assess any experimental error, and the catalytic amount of Pd was adjusted for each catalyst between 0.0001 and 0.01 mol % in order to precisely measure the initial rate for all of the
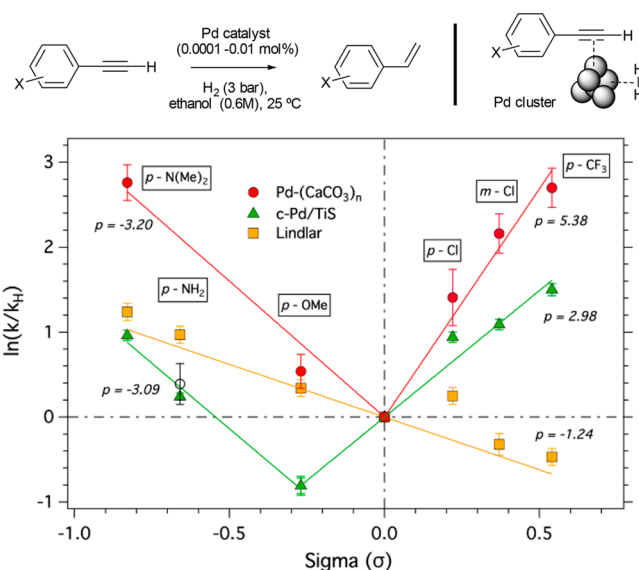
Figure 2. Hammett plots for the hydrogenation of substituted aromatic alkynes catalyzed with Pd–(CaCO$_3$)$_n$ (red), c-Pd/TiS (green), and Lindlar catalyst (orange). The catalytic Pd amount was adjusted for each catalyst in order to precisely measure the initial rate for any substrate. Experiments were made by triplicate. Error bars account for a 5% uncertainty.

substrates under the same reaction conditions. Error bars account for a 5% uncertainty, and the adjusting lines are traced to cross within the points' error bars.

On one hand, the reaction rate with the Lindlar catalyst was always enhanced when electron-donating groups (EDG) were present (see the individual kinetic graphs in Figure S6 and Table S3), showing the classical linear Hammett plot, with $\rho = -1.24$, whereas mildly donating and withdrawing groups did not much affect the reaction rate, in agreement with previous studies.[25] On the other hand, c-Pd/TiS (Figure S7) and Pd–(CaCO$_3$)$_n$ (Figure S8) clearly show a V-shaped Hammett plot. The ρ_{adap} and SEAC values calculated for commercial c-Pd/TiS 6.07 and 98%, respectively, while Pd–(CaCO$_3$)$_n$ shows ρ_{adap} = 8.58 and SEAC = 80%, with the vertexes (least reactive substrates) being 4-ethynylanisole ($\sigma = -0.27$) and phenylacetylene ($\sigma = 0$), respectively. Comparison of the corresponding reaction rates (Table S3) shows that higher rates are obtained for Pd–(CaCO$_3$)$_n$. Thus, it can be concluded that Pd–(CaCO$_3$)$_n$ is a more efficient catalyst, in both reaction rate and substrate scope. It is worth noting that both the c-Pd/TiS and Pd–(CaCO$_3$)$_n$ catalysts show a similar slope for electron-donating groups (−3.09 vs −3.2), which should in principle just be a coincidence but may give some information about the catalytic mechanism, to have in mind for future studies.

It is accepted for the Lindlar catalyst that Pd atoms activate the alkyne and dissociate H$_2$ while the surrounding CaCO$_3$ tunes the Pd electronics and co-adsorbs the slightly acidic terminal alkyne and that Pb acts as an alloying agent to avoid excessive Pd agglomeration and subsequent subsurface hydride formation.[26] In this way, the transfer of substrate electronics to the whole catalytic nanoparticle is minimized.[27] However, the Pd nanoparticles in c-Pd/TiS also show an excellent catalytic activity for the semi-hydrogenation of alkynes,[7] which supports that having small Pd agglomerations is not necessarily detrimental for Pd action.[24] Thus, an electronic transfer

between substrates, H_2, and catalyst may occur, which is the possible reason for the change in mechanism and the V-shaped Hammett plot. Following this rationale, an even better substrate electronics transfer should occur in a smaller nanoparticle, moreover with neighboring $CaCO_3$ around to fix the alkyne, and this is indeed what is observed for Pd−$(CaCO_3)_n$.[24]

Figure 3 shows the Hammett plot obtained for the Ag-catalyzed oxidative coupling of different *para*-substituted
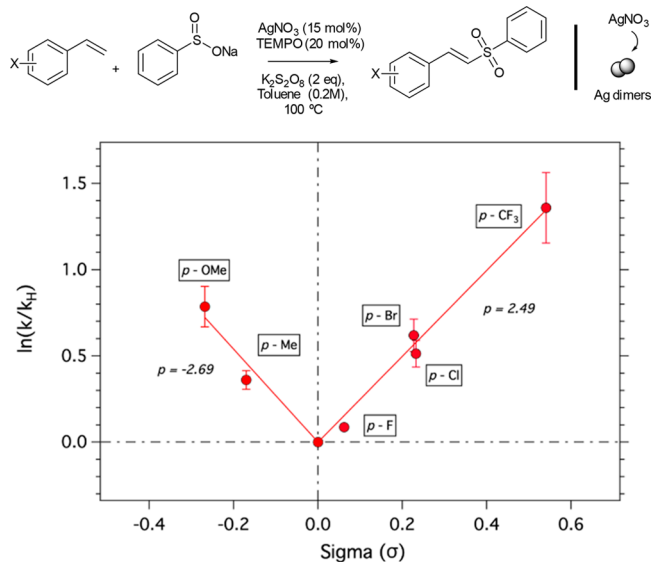
Figure 3. Hammett plot for the Ag-catalyzed oxidative coupling of different *para*-substituted styrenes with sodium benzenesulfone. Experiments were carried out by triplicate. Error bars account for a 5% uncertainty.

styrenes with sodium benzenesulfone, under reported conditions (Figure S9 for individual kinetics).[28] A V-shaped Hammett plot with ρ_{adap} = 5.18 and SEAC = 96% can be seen, which in principle is not related to any metal nanoparticle but to a discrete Ag salt. However, in situ UV−vis emission fluorescence measurements of the reaction mixture show the appearance at the beginning of the reaction of Ag_2 dimers, according to the jellium model (Figure S10),[29] and a kinetic study with different concentrations of $AgNO_3$ reveals that the initial reaction rate (k_0) is exponentially dependent with [Ag], more precisely following a linear dependence with $[Ag]^2$ (Figure S11). UV−vis absorption measurements of the reaction mixture do not show the presence of plasmonic Ag nanoparticles during reaction (Figure S12), and the use of Ag nanoparticles as a catalyst for the coupling reaction with styrene, supported on alumina and whose size is confirmed by UV−visible diffuse reflectance spectrophotometry (Figure S13), does not show any reaction product. These results strongly point to the in situ formation of Ag_2 dimers during reaction, which could be the true catalysts of the reaction and shuttle the styrene electronics for sulfone activation. Metal clusters can transport electrons from one discrete metal atom to another even better than nanoparticles, due to tighter bonds and smaller particle size.[30] In this way, the catalyst can adapt to the different electronic density of the styrene, thus enabling an efficient formation of the radical intermediate regardless of the initial styrene derivative employed.[28]

CONCLUSIONS

We propose here two new parameters, the "adapted sensitivity constant" (ρ_{adap}) and the "substrate electronics adaptability" (SEA), to quantify the potential substrate scope of a catalyst or a reaction. The new parameters are easily obtainable from the Hammett plot: ρ_{adap} indicates the ability of the catalyst or reaction to transform substrates with different electronics, while SEA indicates how similar the reactivities of the substrates are after the mechanism change. We have also shown here two examples currently being explored in our laboratories, i.e., the Pd-catalyzed semi-hydrogenation reaction of aromatic alkynes and the Ag-catalyzed oxidative coupling of styrenes to aryl sulfones, in which metal clusters seem to be the catalytic species able to produce the better values of ρ_{adap} and SEAC, thus a better reaction adaptability to the substrate electronics. Notice that, as far as we know, the concept of catalyst adaptability has traditionally been assigned either to the inherent electronics or to steric factors of the catalyst/ ligands[31−38] but not to substrate electronics.[39,40] Although the better electronic adaptability of soft metal clusters makes chemical sense, of course much more reaction examples have to be studied before having sound conclusions about which catalysts may promote wide scopes. However, this proposal constitutes, in our opinion, a first step toward an easy quantification and comparison of (catalyzed) reactions as a function of substrate electronics adaptability. While it is true that an adaptable catalyst is less selective by definition, many reaction studies require a high level of reactivity and not selectivity, for instance, high-throughput molecular screenings.

ASSOCIATED CONTENT

Supporting Information

The Supporting Information is available free of charge at https://pubs.acs.org/doi/10.1021/acsorginorgau.2c00050.

Experimental details, description of physical techniques, reaction procedures, product characterization, Tables S1−S3, Figures S1−S13, and further references (PDF)

AUTHOR INFORMATION

Corresponding Author

Antonio Leyva-Pérez − *Instituto de Tecnología Química (UPV-CSIC), Universidad Politècnica de València-Consejo Superior de Investigaciones Científicas, 46022 Valencia, Spain;* orcid.org/0000-0003-1063-5811; Phone: +34963877812; Email: anleyva@itq.upv.es; Fax: +34963877809

Authors

Jordi Ballesteros-Soberanas − *Instituto de Tecnología Química (UPV-CSIC), Universidad Politècnica de València-Consejo Superior de Investigaciones Científicas, 46022 Valencia, Spain*

Cristina Bilanin − *Instituto de Tecnología Química (UPV-CSIC), Universidad Politècnica de València-Consejo Superior de Investigaciones Científicas, 46022 Valencia, Spain*

Complete contact information is available at: https://pubs.acs.org/10.1021/acsorginorgau.2c00050

Author Contributions

[†]J.B.-S. and C.B. contributed equally. J.B.-S. performed the hydrogenation reactions and developed the new parameters.

C.B. performed the coupling reactions and developed the new parameters. A.L.-P. conceived the new parameters and coordinated the work, supervised the catalytic part, and wrote the manuscript. CRediT: **Jordi Ballesteros-Soberanas** conceptualization (equal), formal analysis (equal), investigation (equal), methodology (equal), validation (equal); **Cristina Bilanin** investigation (equal), methodology (equal), validation (equal); **Antonio Leyva-Perez** conceptualization (lead), funding acquisition (lead), project administration (lead), supervision (lead), writing-original draft (lead), writing-review & editing (lead).

Notes

The authors declare no competing financial interest.

■ REFERENCES

(1) Erdmann, P.; Greb, L. What Distinguishes the Strength and the Effect of a Lewis Acid: Analysis of the Gutmann-Beckett Method. *Angew. Chem. Int. Ed.* **2022**, *61* (4), e202114550.

(2) Giordano, L.; Akkiraju, K.; Jacobs, R.; Vivona, D.; Morgan, D.; Shao-Horn, Y. Electronic Structure-Based Descriptors for Oxide Properties and Functions. *Acc. Chem. Res.* **2022**, *55* (3), 298−308.

(3) Hammett, L. P. The Effect of Structure upon the Reactions of Organic Compounds. Benzene Derivatives. *J. Am. Chem. Soc.* **1937**, *59*, 96−103.

(4) Hansch, C.; Leo, A.; Taft, R. W. A Survey of Hammett Substituent Constants and Resonance and Field Parameters. *Chem. Rev.* **1991**, *91*, 165−195.

(5) Schreck, J. O. Nonlinear Hammett relationships. *J. Chem. Educ.* **1971**, *48*, 103−107.

(6) Young, P. R.; Jencks, W. P. Separation of Polar and Resonance Substituent Effects in the Reactions of Acetophenones with Bisulfite and of Benzyl Halides with Nucleophiles. *J. Am. Chem. Soc.* **1979**, *101*, 3288−3294.

(7) Stein, A. R.; Tencer, M.; Moffatt, E. A.; Dawe, R.; Sweet, J. Nonlinearity of Hammett.Sigma..Rho. Correlations For Benzylic Systems: Activation Parameters And Their Mechanistic Implications. *J. Org. Chem.* **1980**, *45*, 3539−3540.

(8) Chen, W.; Feng, Y.; Zhang, M.; Wu, J.; Zhang, J.; Gao, X.; He, J.; Zhang, J. Homogeneous Benzoylation of Cellulose in 1-Allyl-3-Methylimidazolium Chloride: Hammett Correlation, Mechanism and Regioselectivity. *RSC. Adv.* **2015**, *5* (72), 58536−58542.

(9) Zdilla, M. J.; Dexheimer, J. L.; Abu-Omar, M. M. Hydrogen Atom Transfer Reactions of Imido Manganese(V) Corroie: One Reaction with Two Mechanistic Pathways. *J. Am. Chem. Soc.* **2007**, *129* (37), 11505−11511.

(10) Neu, H. M.; Yang, T.; Baglia, R. A.; Yosca, T. H.; Green, M. T.; Quesne, M. G.; de Visser, S. P.; Goldberg, D. P. Oxygen-Atom Transfer Reactivity of Axially Ligated Mn(V)-Oxo Complexes: Evidence for Enhanced Electrophilic and Nucleophilic Pathways. *J. Am. Chem. Soc.* **2014**, *136* (39), 13845−13852.

(11) Kalutharage, N.; Yi, C. S. Scope and Mechanistic Analysis for Chemoselective Hydrogenolysis of Carbonyl Compounds Catalyzed by a Cationic Ruthenium Hydride Complex with a Tunable Phenol Ligand. *J. Am. Chem. Soc.* **2015**, *137* (34), 11105−11114.

(12) Pannilawithana, N.; Pudasaini, B.; Baik, M. H.; Yi, C. S. Experimental and Computational Studies on the Ruthenium-Catalyzed Dehydrative C-H Coupling of Phenols with Aldehydes for the Synthesis of 2-Alkylphenol, Benzofuran, and Xanthene Derivatives. *J. Am. Chem. Soc.* **2021**, *143* (33), 13428−13440.

(13) Tejeda-Serrano, M.; Cabrero-Antonino, J. R.; Mainar-Ruiz, V.; López-Haro, M.; Hernández-Garrido, J. C.; Calvino, J. J.; Leyva-Pérez, A.; Corma, A. Synthesis of Supported Planar Iron Oxide Nanoparticles and Their Chemo- and Stereoselectivity for Hydrogenation of Alkynes. *ACS Catal.* **2017**, *7* (5), 3721−3729.

(14) Tejeda-Serrano, M.; Mon, M.; Ross, B.; Gonell, F.; Ferrando-Soria, J.; Corma, A.; Leyva-Pérez, A.; Armentano, D.; Pardo, E. Isolated Fe(III)-O Sites Catalyze the Hydrogenation of Acetylene in Ethylene Flows under Front-End Industrial Conditions. *J. Am. Chem. Soc.* **2018**, *140* (28), 8827−8832.

(15) Oliver-Meseguer, J.; Doménech-Carbó, A.; Boronat, M.; Leyva-Pérez, A.; Corma, A. Partial Reduction and Selective Transfer of Hydrogen Chloride on Catalytic Gold Nanoparticles. *Angew. Chem. Inter. Ed.* **2017**, *56* (23), 6435−6439.

(16) Ertl, P.; Altmann, E.; Mckenna, J. M. The Most Common Functional Groups in Bioactive Molecules and How Their Popularity Has Evolved over Time. *J. Med. Chem.* **2020**, *63* (15), 8408−8418.

(17) Berghauser Pont, L.; Keirsse, J.; Moss, R.; Poda, P.; Robke, L.; Wurzer, S. Developing Blockbuster Drugs: Both Nature and Nurture. *Nat. Rev. Drug. Discovery* **2021**, *20* (6), 421−422.

(18) Bonrath, W.; Medlock, J.; Schutz, J.; Wustenberg, B.; Netscher, T. Hydrogenation in the Vitamins and Fine Chemicals Industry - An Overview. *Hydrogenation*; InTech: 2012. DOI: 10.5772/48751.

(19) Vilé, G.; Almora-Barrios, N.; Mitchell, S.; López, N.; Pérez-Ramírez, J. From the Lindlar Catalyst to Supported Ligand-Modified Palladium Nanoparticles: Selectivity Patterns and Accessibility Constraints in the Continuous-Flow Three-Phase Hydrogenation of Acetylenic Compounds. *Chem. - Eur. J.* **2014**, *20* (20), 5926−5937.

(20) Witte, P. T.; Berben, P. H.; Boland, S.; Boymans, E. H.; Vogt, D.; Geus, J. W.; Donkervoort, J. G. BASF NaNoSelect^{TM} Technology: Innovative Supported Pd- and Pt-Based Catalysts for Selective Hydrogenation Reactions. *Top. Catal.* **2012**, *55*, 505−511.

(21) Ballesteros-Soberanas, J.; Hernández-Garrido, J. C.; Cerón-Carrasco, J. P.; Leyva-Pérez, A. Selective Semi-Hydrogenation of Internal Alkynes Catalyzed by Pd-CaCO3 Clusters. *J. Catal.* **2022**, *408*, 43−55.

(22) Ballesteros-Soberanas, J.; Carrasco, J. A.; Leyva-Pérez, A. Parts-Per-Million of Soluble Pd(0) Catalyze the Semi-Hydrogenation Reaction of Alkynes to Alkenes. *J. Org. Chem.* **2022**, DOI: 10.1021/acs.joc.2c00616.

(23) Furukawa, S.; Komatsu, T. Selective Hydrogenation of Functionalized Alkynes to (*E*)-Alkenes, Using Ordered Alloys as Catalysts. *ACS Catal.* **2016**, *6* (3), 2121−2125.

(24) Delgado, J. A.; Benkirane, O.; Claver, C.; Curulla-Ferré, D.; Godard, C. Advances in the Preparation of Highly Selective Nanocatalysts for the Semi-Hydrogenation of Alkynes Using Colloidal Approaches. *Dalton Trans.* **2017**, *46*, 12381−12403.

(25) Fiorio, J. L.; Gonçalves, R. V.; Teixeira-Neto, E.; Ortuño, M. A.; López, N.; Rossi, L. M. Accessing Frustrated Lewis Pair Chemistry through Robust Gold@N-Doped Carbon for Selective Hydrogenation of Alkynes. *ACS Catal.* **2018**, *8* (4), 3516−3524.

(26) Albers, P. W.; Möbus, K.; Frost, C. D.; Parker, S. F. Characterization of β-Palladium Hydride Formation in the Lindlar Catalyst and in Carbon-Supported Palladium. *J. Phys.Chem. C* **2011**, *115* (50), 24485−24493.

(27) Fukuda, T. Partial Hydrogenation of 1,4-Butynediol. II. On the Role of Calcium Carbonate as a Carrier of the Palladium Catalyst. *Bull. Chem. Soc. Jpn.* **1958**, *31*, 343−347.

(28) Gui, Q.; Han, K.; Liu, Z.; Su, Z.; He, X.; Jiang, H.; Tian, B.; Li, Y. E -Selective Synthesis of Vinyl Sulfones via Silver-Catalyzed Sulfonylation of Styrenes. *Org. Biomol. Chem.* **2018**, *16* (32), 5748−5751.

(29) Oliver-Meseguer, J.; Cabrero-Antonino, J. R.; Domínguez, I.; Leyva-Pérez, A.; Corma, A. Small Gold Clusters Formed in Solution Give Reaction Turnover Numbers. *Science* **2012**, *338*, 1452−1455.

(30) Boronat, M.; Leyva-Pérez, A.; Corma, A. Theoretical and Experimental Insights into the Origin of the Catalytic Activity of Subnanometric Gold Clusters: Attempts to Predict Reactivity with

Clusters and Nanoparticles of Gold. *Acc. Chem. Res.* **2014**, *47* (3), 834−844.

(31) Zalubovskis, R.; Bouet, A.; Fjellander, E.; Constant, S.; Linder, D.; Fischer, A.; Lacour, J.; Privalov, T.; Moberg, C. Self-Adaptable Catalysts: Substrate-Dependent Ligand Configuration. *J. Am. Chem. Soc.* **2008**, *130* (6), 1845−1855.

(32) Rascón, F.; Wischert, R.; Copéret, C. Molecular Nature of Support Effects in Single-Site Heterogeneous Catalysts: Silica vs. Alumina. *Chem. Sc.* **2011**, *2*, 1449−1456.

(33) Gardiner, M. G.; Ho, C. C.; Mackay, F. M.; McGuinness, D. S.; Tucker, M. Selective and Adaptable Access to N, N′-Asymmetrically Substituted Imidazol-2-Ylidene Bis-NHC Ligands: Pd(Ii) Complexes Featuring Wide Variation in N-Alkyl and Aryl Steric Bulk. *J. Chem. Soc., Dalton Trans.* **2013**, *42* (20), 7447−7457.

(34) Lee, C. I.; Hirscher, N. A.; Zhou, J.; Bhuvanesh, N.; Ozerov, O. v. Adaptability of the SiNN Pincer Ligand in Iridium and Rhodium Complexes Relevant to Borylation Catalysis. *Organometallics* **2015**, *34* (13), 3099−3102.

(35) Morisaki, K.; Sawa, M.; Yonesaki, R.; Morimoto, H.; Mashima, K.; Ohshima, T. Mechanistic Studies and Expansion of the Substrate Scope of Direct Enantioselective Alkynylation of α-Ketiminoesters Catalyzed by Adaptable (Phebox)Rhodium(III) Complexes. *J. Am. Chem. Soc.* **2016**, *138* (19), 6194−6203.

(36) Vereshchuk, N.; Matheu, R.; Benet-Buchholz, J.; Pipelier, M.; Lebreton, J.; Dubreuil, D.; Tessier, A.; Gimbert-Suriñach, C.; Ertem, M. Z.; Llobet, A. Second Coordination Sphere Effects in an Evolved Ru Complex Based on Highly Adaptable Ligand Results in Rapid Water Oxidation Catalysis. *J. Am. Chem. Soc.* **2020**, *142* (11), 5068−5077.

(37) Wang, X.; Han, Z.; Wang, Z.; Ding, K. A Type of Structurally Adaptable Aromatic Spiroketal Based Chiral Diphosphine Ligands in Asymmetric Catalysis. *Acc. Chem. Res.* **2021**, *54* (3), 668−684.

(38) Diéguez, M.; Pàmies, O.; Moberg, C. Self-Adaptable Tropos Catalysts. *Acc. Chem. Res.* **2021**, *54* (16), 3252−3263.

(39) Aponick, A.; Biannic, B.; Jong, M. R. A Highly Adaptable Catalyst/Substrate System for the Synthesis of Substituted Chromenes. *Chem. Commun.* **2010**, *46* (36), 6849−6851.

(40) Sawatlon, B.; Wodrich, M. D.; Corminboeuf, C. Probing Substrate Scope with Molecular Volcanoes. *Org. Lett.* **2020**, *22* (20), 7936−7941.